ANALYTICAL MODELLING OF THE VARYING BENDING STIFFNESS INSIDE THE BOUNDARY LAYER OF CABLES

Francesco FOTI[a], Luca MARTINELLI[a], Vincent DENOËL[b]
[a]Department of Civil and Environmental Engineering, Politecnico di Milano, Italy
[b]Structural & Stochastic Dynamics, University of Liège, Belgium
francesco.foti@polimi.it, luca.martinelli@polimi.it, v.denoel@uliege.be

Introduction

In the present paper, a novel model for a shallow cable with small bending stiffness subjected to transverse loading conditions is presented. The proposed model is based on a simple yet accurate phenomenological description of the non-linear moment-curvature law of stranded cables. Numerical solutions are first compared to experimental results of the literature, to assess the validity of the proposed formulation. Parametric analyses are then carried out to investigate the effect of different non-dimensional variables controlling the bending stiffness variation within the boundary layers.

BACKGROUND

Bending fretting fatigue of cables is a major concern in the design and retrofitting of many structures, such as electrical transmission lines, suspended and stayed bridges and mooring systems for offshore engineering applications. Fretting fatigue failures typically occur close to suspension or anchoring devices, where the stress-strain state is markedly different with respect to the one predicted by the perfectly flexible structural models, often adopted to characterize the large-scale static and dynamic response of cables (e.g. [1]). In fact, within these critical regions, also termed *bending boundary layers* (see e.g. [2]), transverse oscillations due to environmental loads can induce both significant alternate bending stresses and relative displacements between the wires of the cable.
The onset and propagation of relative displacements between the wires of the cable is controlled by the activation of complex internal sticking/sliding contact patches, that makes the bending response of the cable inherently non-linear and non-holonomic and determines a transition from a full-sticking to a full-slipping behavior of the cable cross sections for increasing values of the curvature (see e.g. [3-5]). Differences between the bending stiffness associated to the full-sticking and full-slipping conditions are typically of two orders of magnitude for multi-layer stranded cables. Accurate modeling of the cable bending behavior within the boundary layers is a fundamental prerequisite to a deeper comprehension of bending fretting fatigue phenomena.
Being typically developed under the assumption of linearly elastic bending behavior (see e.g. [6, 7]), available analytical models dealing with the determination of the stress-strain state within the cable boundary layers fail to capture the effects related to the variations of bending stiffness with the curvature.
This paper presents a novel model for a suspended cable with small bending stiffness subject to transverse loading conditions. The proposed model is based on a simple yet accurate smooth moment-curvature constitutive law that allows to account for non-linearities due to the onset and propagation of relative displacements between the wires of the cable.
Numerical solutions are first compared to available experimental results of the literature, to assess the validity of the proposed formulation. A minimal set of non-dimensional variables controlling the bending stiffness variation within the boundary layers is identified. Parametric analyses are then carried out to investigate the role played by these non-dimensional variables on the solution of the mechanical problem.

THE CONSIDERED PROBLEM

In this paper, the static response of a tensioned cable suspended to horizontal supports is investigated focusing on two archetypal transverse loading conditions (see Fig. 1): (a) uniformly distributed force per unit of length w (e.g. cable self-weight), and (b) weightless cable subject to a concentrated force F applied at the midspan. The first loading condition is typically considered to determine the static equilibrium configuration of suspended cables, such as overhead electrical line conductors and guard wires, subject to dead loads and the static component of wind forces. The second loading case, instead, is herein considered to reproduce bending tests on short cable specimens (with length in the order of 1-5 m) that have been often reported in the literature [3, 8].

The cable is assumed to be clamped at both ends (i.e. rotations of the end sections are assumed to be perfectly restrained) and axially inextensible. Focusing on monotonic loading conditions, the bending stiffness (EI) of the cable cross sections is assumed to be a non-linear single-valued function of the cable curvature χ, i.e. $EI = EI(\chi(s))$ where s is an arc-length coordinate spanning the length l of the cable.

Both loading conditions (a) and (b) lead to a structural problem symmetric with respect to the cable midspan and can be described within a unitary framework. To this aim let us denote as H and V, respectively, the horizontal and vertical reactions of the supports. The horizontal reaction is assumed as a known parameter of the problem and is expressed as a ratio of the Rated Tensile Strength (RTS) of the cable: $H = \eta_0 \, RTS$. The vertical reaction is easily calculated, by simultaneously considering the two loading conditions (a) and (b), as: $V = (wl + F)/2$.

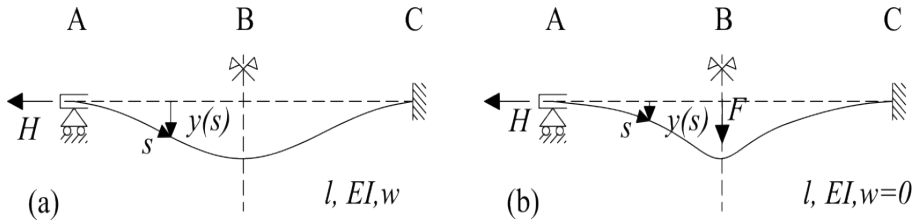

Figure 1. Considered problems: (a) suspended cable subject to the constant load per unit of length w, (b) weightless (w=0) cable subject to a concentrated force F applied at the midspan. In both cases the cable is assumed to be pre-tensioned and the horizontal force at the supports is denoted as H.

The equilibrium equations

Local and global equilibrium equations can be obtained by considering, respectively, an infinitesimal (Fig. 2(a)) or finite (Fig. 2(b)) portion of the cable (see e.g. [1, 6]). Starting from Fig. 2(b), the axial (N) and shear (T) force can be evaluated as:

$$N = H\cos(\theta) + (V - w\,s)\sin(\theta) \tag{1}$$

$$T = H\sin(\theta) - (V - w\,s)\cos(\theta) \tag{2}$$

where $\theta(s)$ denotes the inclination angle of the cable centerline to the horizontal direction.

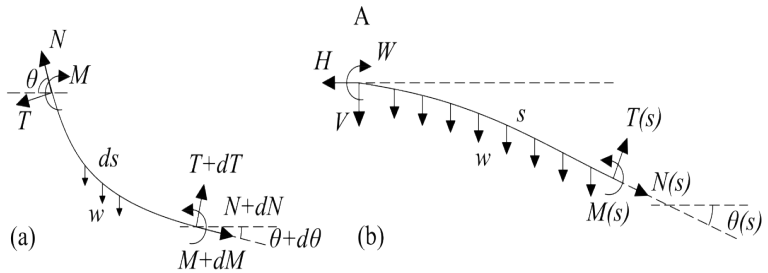

Figure 2. Local (a) and global (b) equilibrium of the cable.

Equilibrium with respect to the rotation of an infinitesimal segment of the cable (see Fig. 2(a)), then, allows to relate the first derivative of the bending moment with respect to the arc-length coordinate s to the shear force:

$$dM/ds = -T \tag{3}$$

The cross-sectional bending stiffness

Metallic cables are typically made of helical wires, twisted around an initially straight core and gathered together in concentric layers. The bending stiffness of the cable is mainly controlled by the evolution of frictional interaction phenomena between adjacent wires. When a cable is bent, indeed, interwire friction forces are initially large enough to prevent any relative displacement between the wires. As a result, the wires can be considered as perfectly stuck together (*full-stick* state) and the bending stiffness attains its maximum theoretical value EI_{max}, which is of the same order of magnitude as the one of a solid circular cross section with the same diameter as the cable. The friction forces, however, can increase only up to a maximum value, that depends on the geometry of the wires, the value of the axial force of the cable and the interwire friction coefficient. By monotonically increasing the value of the bending curvature χ, the effects of the friction forces can be overcome allowing for the relative sliding of the wires. Progressive sliding of the wires determines a reduction of the cross-sectional tangent bending stiffness. When all the wires are in the sliding state (*full-slip* state) the tangent bending stiffness reaches its minimum theoretical value EI_{min}, which is of the same order of magnitude as the one of a bundle of independently bent wires.
Closed form analytical expressions have been proposed in the literature to evaluate EI_{max} and EI_{min} on the basis of the sole knowledge of the material and geometrical properties of the wires. These expressions are mostly based on the assumption of rigid contact interfaces between the wires and lead to fairly good predictions of EI_{min}. The maximum theoretical bending stiffness EI_{max}, on the other hand, is typically overestimated as a consequence of neglecting the deformability of the internal contact interfaces between the wires [8, 9]. On a practical ground, an effective maximum value ($EI_{max,ef}$) of the cross sectional bending stiffness can be conveniently defined as [10, 11]:

$$EI_{max,ef} = \beta EI_{max} \tag{4}$$

where β is a stiffness reduction factor ($0<\beta\leq1$). Typical values of β can be assumed in the range β = 0.5-0.95 for overhead electrical line conductors. Different models have been developed in the literature to describe the non-linear transition from the full-stick (small curvature regime) to the full-slip (large curvature regime) state. Most of them rely on a wire-by-wire modeling strategy that leads to a moment-curvature (M-χ) constitutive law that can be expressed in the form:

$$M = EI_{min}\,\chi + M^{add}(\chi) \tag{5}$$

where the linear term corresponds to the theoretical response of the cable under the full-slip assumption, while the non-linear term $M^{add}(\chi)$ accounts for the additional contribution to the bending moment of the cable coming from the axial force of each wire. Starting from the formulation proposed in [4, 5, 10, 11], a smooth moment-curvature (M-χ) constitutive law is herein defined as:

$$M = -EI_{max,ef}\,\{\gamma^2\,\chi + (1-\gamma^2)\,\chi_0\,\mathrm{sgn}(\chi)\,[1-\exp(-|\chi|/\chi_0)]\} \tag{6}$$

where $\chi = d\theta/ds$ is the bending curvature of the cable, $\gamma^2 = EI_{min}/EI_{max,ef}$ (values of γ^2 are typically in the order of few percent) and χ_0 is a reference curvature value related to the activation of gross-sliding phenomena between the wires of the strand. This value is typically associated to the onset of gross-

sliding between the wires of the outermost layer of the strand and the wires of the penultimate one. The following equation has been proposed in [10, 11] to calculate χ_0:

$$\chi_0 = c_0 \, \mu \, \eta \tag{7}$$

where μ is the interwire friction coefficient (an indicative range of values for μ can be 0.15-0.7, with lower values associated to new and well-lubricated cables and higher values associated to old or non-lubricated ones), c_0 is a coefficient depending only on the internal geometry of the strand (typical values of c_0 are in the range 0.1-0.2 m^{-1}, see [11]), and η is the ratio between the axial force of the cable and its Rated Tensile Strength (*RTS*), i.e: $\eta(s) = N(s)/RTS$.

The boundary value problem

By recalling that $\chi = d\theta/ds$, derivation of Eq. (6) with respect to the arc-length coordinate s yields:

$$dM/ds = -EI_{max,ef} [\gamma^2 + (1 - \gamma^2) \exp(-|d\theta/ds| / \chi_0)] \, d^2\theta/ds^2 \tag{8}$$

By combining Eqs. (2), (3) and (8) the following non-linear second order differential equation is obtained:

$$EI_{max,ef} [\gamma^2 + (1 - \gamma^2) \exp(-|d\theta/ds| / \chi_0)] \, d^2\theta/ds^2 = H \sin(\theta) - (V - w\, s) \cos(\theta) \tag{9}$$

Due to the symmetry of the considered problems, the equation (9) can be integrated over the interval $s \in [0, l/2]$ along with the boundary conditions:

$$\theta(s=0) = \theta(s=l/2) = 0 \tag{10}$$

Eqs. (9) and (10) define a boundary value problem that can be solved to evaluate the inclination angle $\theta(s)$. Once $\theta(s)$ is known, the internal forces (N, T) and bending moment (M) distributions can be retrieved through eqs. (1), (2) and (3) (or (6)).

THE NON-DIMENSIONAL FORMULATION

In this Section, the considered problem is re-stated in a more convenient non-dimensional form. To this aim, let us introduce the non-dimensional arc-length coordinate:

$$\xi = s/l, \quad \xi \in [0, 1/2] \tag{11}$$

Substitution of Eq. (11) in (9) yields the non-dimensional equation:

$$\varepsilon^2 [\gamma^2 + (1 - \gamma^2) \exp(-|\Theta'| / X_0)] \, \Theta'' = \sin(\Theta) - [(\omega + \psi)/2 - \omega\xi] \cos(\Theta) \tag{12}$$

where $\Theta = \theta(s(\xi))$, a prime denotes differentiation with respect to ξ and the following non-dimensional variables have been introduced:

$$\varepsilon^2 = EI_{max,ef} / (Hl^2), \quad X_0 = \chi_0 l, \quad \omega = wl/H, \quad \psi = F/H \tag{13}$$

Eq. (12) should be integrated over the interval $\xi \in [0, 1/2]$ with boundary conditions (cf. Eq. (10)):

$$\Theta(\xi=0) = \Theta(\xi=1/2) = 0 \tag{14}$$

The main features of the solutions of the boundary value problem (12)-(14) depend on the order of magnitude of the non-dimensional parameters ε^2, X_0, ω, and ψ. As an example, let us consider a widespread class of overhead electrical conductors made of a steel core surrounded by one or more layers of aluminum wires, i.e. the Aluminum Conductors Steel Reinforced (ACSR). Focusing on ACSR with diameter in the range 1.5-4.5 cm, strung at 10%-50% of their Rated Tensile Strength (RTS) the non-dimensional bending stiffness parameter ε can be in the range 10^{-4}-10^{-2} for spans ranging from 50 to 250 m. Larger values of ε, in the order of 10^{-2}-10^{-1} can be attained in short experimental testing spans (with lengths in the order of 1-5 m). Typical values of the non-dimensional reference curvature for the onset of gross sliding phenomena, X_0, are in the range 10^{-1}-10^{1} for spans ranging from 50 to 250 m. In testing spans ranging from 1 to 5 m, instead, X_0 is in the order of 10^{-3}-10^{-1}. The non-dimensional catenary parameter ω can be in the order of 10^{-2}-10^{0} for spans ranging from 50 to 250 m. Significantly smaller values, in the order of 10^{-4}-10^{-2}, instead, are associated to testing spans ranging from 1 to 5 m. Finally, the non-dimensional transverse load parameter ψ has been typically assumed in the order of 0.03-0.125 in experimental tests reported in the literature [3, 8].
It is worth noting that the small number ε^2 multiplying the highest order derivative in Eq. (12) makes the boundary value problem (12)-(14) singularly perturbed and hints the existence of boundary layers in the static equilibrium configuration. These boundary layers have been already studied in the literature under the assumption of constant bending stiffness EI (e.g. [6, 7]). The latter case can be recovered as a special case of the proposed formulation by letting the reference curvature χ_0 tend to infinite (such that $EI \rightarrow EI_{max,ef}$) or to zero (such that $EI \rightarrow EI_{min}$). Consideration of the smallness of the parameter ε^2 naturally paves the way for solutions strategies based on perturbation techniques and ongoing research is oriented towards this goal. The present paper, instead, focuses on preliminary numerical simulations with a twofold goal: (1) showing the soundness of the proposed model and (2) investigate the role of different non-dimensional groups on the bending stiffness variations along the cable. Special care will be taken within this context, to highlight stiffness transitions within the boundary layers, that cannot be captured by available analytical models of the literature based on the simplifying constant stiffness assumption.

APPLICATION EXAMPLES

In this Section, the proposed model is first applied to simulate a well-documented bending test of the literature [8]. Parametric analyses are then carried out to investigate the role played by different non-dimensional variables controlling the bending stiffness variation within the boundary layers. In all cases, solutions of the boundary value problem (12)-(14) have been obtained through a numerical solver based on a collocation algorithm.

Comparison with experimental results

Baumann and Novak [8] reported results of a bending test performed on a short stretch (2 m in length) of an ACSR Drake. The cable was first subjected to a horizontal force H=0.2·RTS and then loaded with a transverse force F growing from zero up to the maximum value 0.05·H and applied at the midspan as it is schematically depicted in Fig. 1(b). Geometric and mechanical parameters of the ACSR Drake have been calculated according to the ASTM standard [12]. They are listed in the following: diameter D=2.81 cm, Rated Tensile Strength RTS=138 kN, mass per unit of length m=1.626 kg/m, maximum value of the bending stiffness EI_{max}=1487 Nm^2, minimum value of the bending stiffness EI_{min}=42.9 Nm^2. Notice that a slightly lower value of EI_{max} is reported in [8]. This difference can be due to slight differences on the geometric and mechanical properties of the wires. Based on the previously reported values and assuming a unitary stiffness reduction parameter (i.e. β=1), the ratio γ^2 turns out to be equal to $\gamma^2 = EI_{min}/ EI_{max,ef}$ =0.0289. The construction parameter c_0 has been calculated based on the formulation presented in [4] and is equal to 0.161 m^{-1}. All simulations have been run by assuming an interwire friction coefficient μ=0.5 ,coherently with the assumption reported in [8].

Fig. 3(a) shows the static equilibrium configuration under the maximum transverse load $F= 0.05 \cdot H$: the non-dimensional transverse displacements $y^*=y(s(\xi))/l$ are plotted versus the non dimensional arc-length coordinate $\xi \in [0, 1/2]$. The outcomes of the proposed model are compared to both experimental data and results of a three-dimensional finite element model from [8] showing a good agreement. The two curves obtained from the application of the proposed model under the simplifying assumption of constant bending stiffness equal to EI_{min} and EI_{max} are also shown in Fig. 3(a). Fig. 3(b) shows the variation of the cable non-dimensional bending stiffness ($EI^*=EI/(Hl^2)$) predicted by the proposed model over the interval $\xi \in [0, 1/2]$.

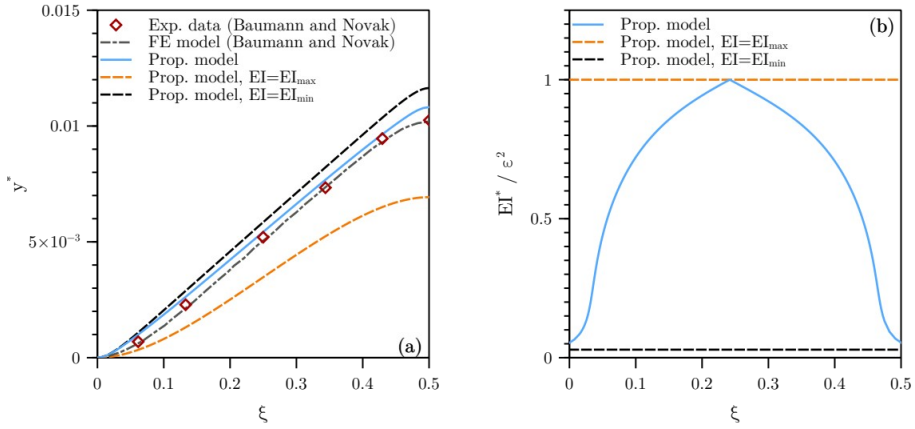

Figure 3. (a) Static equilibrium configuration of a 2m long Drake ACSR subject to H=0.2RTS and F=0.05H. The outcomes of the proposed model are compared to experimental data and results of a Finite Element (FE) model from [8]. (b) Calculated non-dimensional bending stiffness distribution over the interval $\xi \in [0, 1/2]$.

Parametric analyses

Parametric analyses have been carried out by considering the loading condition depicted in Fig. 1(a), which is relevant e.g. for the assessment of overhead electrical line spans under self-weight and static wind loading conditions. The analyses have been carried out by assuming $\varepsilon=10^{-2}$, $\gamma^2=0.0289$, $\eta_0=H/RTS=0.2$ and interwire friction coefficient $\mu=0.5$. These values can be considered as representative of suspended cables employed in overhead electrical lines. Results are shown in Fig. 4 in terms of the inclination angle $\Theta(\xi)$, the non-dimensional bending stiffness $EI^*=EI/(Hl^2)$ and the static equilibrium configuration $y^*(\xi)$.

Figures 4(a)-(c) show the results obtained by assuming different values of the non-dimensional catenary parameter $\omega = wl/H$ (governing the tautness of the cable) and a constant value $X^*_0=c_0\mu\eta l=1.61$ in order to calculate the reference non-dimensional curvature value $X_0 = \chi_0 l = X^*_0 N(s(\xi))/RTS = X^*_0 \eta(\xi)$. As expected, by increasing the parameter ω the static equilibrium configuration significantly varies (see Figs. 4(a) and 4(c)).More interestingly, Fig. 4(b) shows that different values of ω are associated to significantly different bending stiffness distributions along the length of the cable. In this plot there are two ranges of interest: in-span ($\xi \sim 0.5$) and in the boundary layer ($\xi << 1$). When EI^*/ε is equal to 1, $EI= EI_{max,ef}$ and the curvature of the cable is smaller than the threshold corresponding to gross sliding. In all considered cases, there is at least one abscissa where $EI^*/\varepsilon=1$. It corresponds to the inflexion point: the curvature is negative on the left of this point and is positive on the right. For a small catenary parameter ω, the cable is rather flat, with a small curvature and the in-span bending stiffness is close to $EI_{max,ef}$, see values close to $\xi=0.5$. On the contrary, for a significantly sagging cable (larger catenary parameter ω), the in-span curvature is so large that the bending stiffness is also reduced in the span, see for instance $EI^*/\varepsilon \sim 0.2$ for $\omega=1$. In the boundary layer, in the neighbourhood of the origin, the curvature is negative due to the boundary condition. For all considered cases, the curvature is so large (in absolute value) that the bending stiffness corresponds to the minimum value. When $\omega=0.1$ or $\omega=1$ the behaviour in the boundary layer is the same exhibiting a so-called 2-deck boundary layer approximation. The extent of the boundary layer is much larger for

ω=0.01 (the highly taut cable). This numerical simulation indicates that larger axial forces in the cable tend to increase the extent of the boundary layer, which generalizes what is known for cables with constant bending stiffness [6].
Figures 4(d)-(f) show the results obtained by assuming different values of X^*_0 and a constant value of the non-dimensional catenary parameter, namely ω =0.01. As it can be noticed by Figs. 4(d) and 4(f), changes in X^*_0 do not significantly affect the deformed shaped of the cable, which is already highly taut. The pattern of the boundary layer solution is highly dependent on X^*_0 : for a large threshold the most important part of the cable is under low curvature, as expected and the maximum bending stiffness is observed along almost the whole length of the cable. Conversely, for a small threshold, the profile of the bending stiffness is very much alike the profile obtained for slacker cables, i.e. with a shorter boundary layer, a sharp transition and a smaller in-span bending stiffness.

CONCLUSIONS

In this paper, we have unveiled the specific nature of the 2-deck boundary layer in stranded cables which exhibit a smooth transition from full bending stiffness to reduced bending stiffness, as a result of the gross sliding of the different wires making up the cross section. Numerical simulations have been used for this study. They highlight the main features of the boundary layer solution. At this stage, it is too early to derive simple analytical formulations to predict the different response profiles. However, this analysis shall serve as a solid basis to inspire a perturbation analysis solution. It is clear though, that the profile of the response is the neighbourhood of the support is highly dependent on the tautness parameter and the geometrical parameters of the cable. These simulations and the arguments developed in the scope of this paper tend to question the systematic use of experiments with a systematic measurement at a distance of 89 mm from the support to describe or quantify the response of the cable. Indeed, a fixed distance, which seems appealing for codification purposes, could certainly fall inside or outside the boundary layer, whose profile is furthermore highly dependent on the considered configuration. The use of a systematic distance seems therefore inappropriate to capture all possible configuration. Further studies are required to derive clean 2-deck matched asymptotic solutions and eventually derive the exact conditions under which the 89-mm is appropriate to represent the actual cable behaviour.

REFERENCES

[1] H. Irvine, 1981, *Cable Structures,* Mit Press Series in Structural Mechanics.

[2] J.G.A. Croll, 2000, “Bending boundary layers in tensioned cables and rods”, *Applied Ocean Research*, vol. 12, 241-253.

[3] K.O. Papailiou, 1997, “On the bending stiffness of transmission line conductors”, *IEEE Trans. Pow. Del.*, vol. 12, 1576-1588.

[4] F. Foti, L. Martinelli, 2016, “Mechanical modeling of metallic strands subjected to tension, torsion and bending”, Int. J. Sol. Struct., vol. 91, 1-17.

[5] F. Foti, L. Martinelli, 2016, “An analytical approach to model the hysteretic bending behavior of spiral strands”, *Appl. Math. Mod.*, vol. 40, 6451-6467.

[6] V. Denoël, E. Detournay, 2010, “Multiple scales solution for a beam with a small bending stiffness”, *J. Eng. Mech.*, vol. 136, 69-77.

[7] V. Denoël, T. Canor, 2013, “Patching asymptotics solution of a cable with a small bending stiffness”, *J. Struct. Eng.*, vol. 139, 180-187.

[8] R. Baumann, P. Novak, 2017, "Efficient computation and experimental validation of ACSR overhead line conductors under tension and bending", *Cigre Science and Engineering*, vol. 9, 5-16.

[9] J.P. Paradis, F. Legeron, 2011, "Modelling of the free bending behavior of a multilayer cable taking into account the tangential contact compliance of contact interfaces", *Conf. Proc., ISCD 2011 - 9th Int. Symposium on Cable Dynamics, 18-20 October 2011, Shanghai, China,* 8 pages.

[10] F. Foti, L. Martinelli, 2018, "A unified analytical model for the self-damping of stranded cables under aeolian vibrations", *J. Wind Eng. Ind. Aerodyn*., vol. 176, 225-238.

[11] F. Foti, L. Martinelli, 2018, "An enhanced unified model for the self-damping of stranded cables under aeolian vibrations ", *J. Wind Eng. Ind. Aerodyn*., vol. 182, 72-86.

[12] ASTM – American Society for Testing Materials, 1985, *ASTM Standards on Metallic Electrical Conductors*, PCN 01-020385-22.

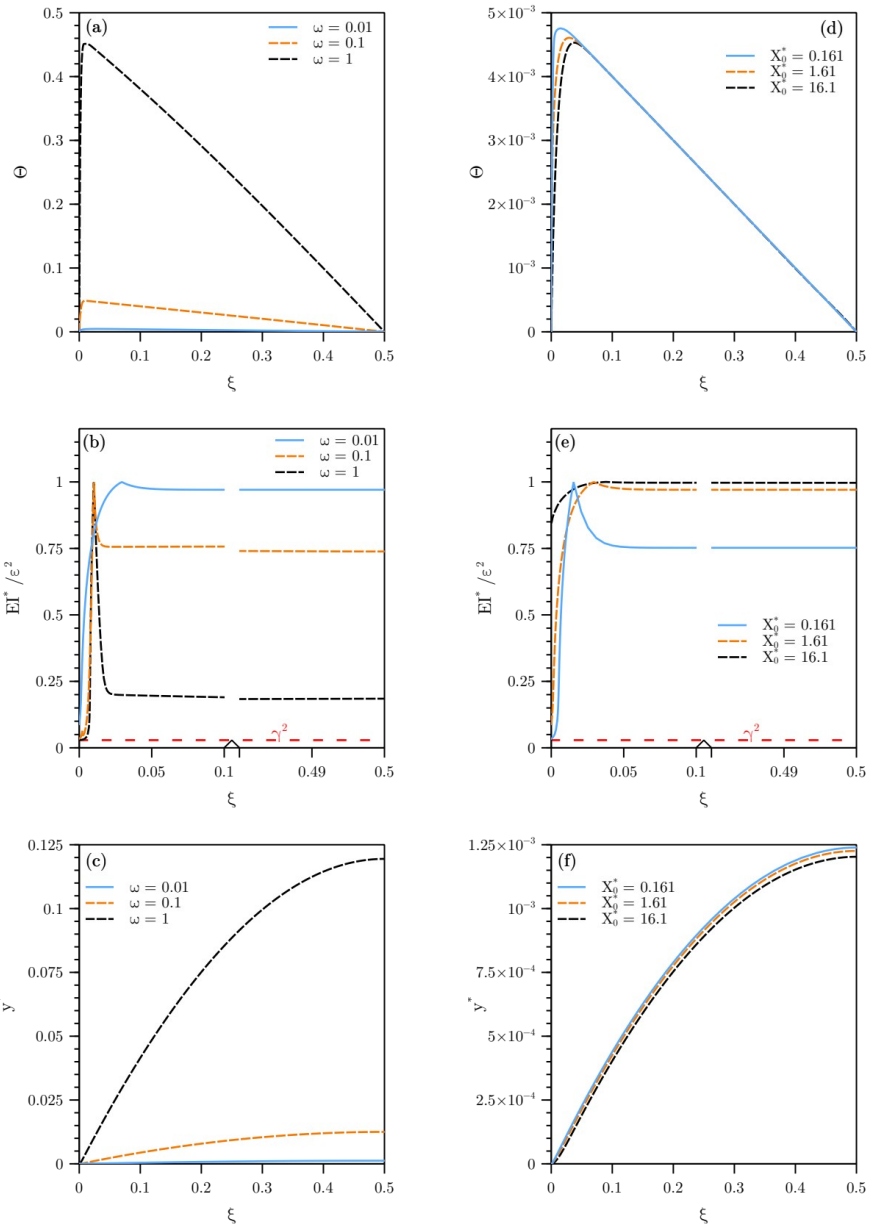

Figure 4. Results of the parametric analyses. Figures (a)-(c) are calculated for a constant value X^*_0=1.61 and different values of the non-dimensional catenary parameter ω. Figures (d)-(f) are calculated for a constant value ω=0.01 and different values of X^*_0.